Journal of Alloys and Compounds 509 (2011) 4595–4602

Contents lists available at ScienceDirect

Journal of Alloys and Compounds

journal homepage: www.elsevier.com/locate/jallcom

Interfacial reactions and mechanical properties between Sn–4.0Ag–0.5Cu and Sn–4.0Ag–0.5Cu–0.05Ni–0.01Ge lead-free solders with the Au/Ni/Cu substrate

Yee-Wen Yen[a,b,*], Yu-Cheng Chiang[c], Chien-Chung Jao[d], Da-Wei Liaw[a], Shao-cheng Lo[b], Chiapyng Lee[c]

[a] Department of Materials Science and Engineering, National Taiwan University of Science and Technology, Taipei 10672, Taiwan, ROC
[b] Graduate Institute of Engineering, National Taiwan University of Science and Technology, Taipei 10672, Taiwan, ROC
[c] Department of Chemical Engineering, National Taiwan University of Science and Technology, Taipei 10672, Taiwan, ROC
[d] Department of Chemical and Materials Engineering, Ta Hwa Institute of Technology, Hsinchu 30703, Taiwan, ROC

ARTICLE INFO

Article history:
Received 29 November 2010
Received in revised form 12 January 2011
Accepted 15 January 2011
Available online 22 January 2011

Keywords:
Sn–4.0Ag–0.5Cu and Sn–4.0Ag–0.5Cu–0.05Ni–0.01Ge lead-free solders
Au/Ni/Cu multi-layer
Intermetallic compounds
Diffusion-controlled
Mechanical strength

ABSTRACT

Sn–4.0Ag–0.5Cu (SAC) and Sn–4.0Ag–0.5Cu–0.05Ni–0.01Ge (SACNG) lead-free solders reacting with the Au/Ni/Cu multi-layer substrate were investigated in this study. All reaction couples were reflowed at 240 and 255 °C for a few minutes and then aged at 150 °C for 100–500 h. The (Cu, Ni, Au)$_6$Sn$_5$ phase was formed by reflowing for 3 min at the interface. If the reflowing time was increased to 10 min, both (Cu, Ni, Au)$_6$Sn$_5$ and (Ni, Cu, Au)$_3$Sn$_4$ phases formed at the interface. The AuSn$_4$ phase was found in the solder for all reaction couples. An addition of Ni and Ge to the solder does not significantly affect the IMC formation. After a long period of heat-treatment, the thickness of the (Cu, Ni, Au)$_6$Sn$_5$ and (Ni, Cu, Au)$_3$Sn$_4$ phases increased and the intermetallic compounds (IMCs) growth mechanism obeyed the parabolic law and the IMC growth mechanism was diffusion-controlled. The mechanical strengths for both the soldered joints decreased with increasing thermal aging time. The SACNG/Au/Ni/Cu couple had better mechanical strength than that in the SAC/Au/Ni/Cu couple.

1. Introduction

Due to the toxicity of lead (Pb) and its harm to the environment and human health, Sn–Pb solders are not allowed to be used in electronic products [1–4]. Lead-free solders have become an important issue in electronic packaging industry [5,6]. Sn–Ag–Cu alloys are very suitable substitutes for Sn–Pb solders because they have better mechanical properties and reliability after soldering [7]. However, the liquidus temperature of the Sn–Ag–Cu solders is about 30 °C higher than that of the Sn–37Pb solder. The higher soldering temperature would bring serious oxidation problem to the solder surface and decrease the wettability between the solder and substrate. Cho et al. found that a small amount of Ge added into the Sn–Ag–Cu solders would inhibit the oxidation problem and increase the solder joint mechanical strength [8]. The Au/Ni multilayer structure is commonly used as the under bump metallization (UBM) in the ball grid array (BGA) and flip chip (FC) bonding technique. The Au layer can prevent oxidation, enhance the wettability, and the Ni layer acts as a diffusion barrier to prevent the rapid reaction between the solder and the Cu substrate [9,10].

Massive research groups have studied interfacial reactions between Sn–Ag and Sn–Ag–Cu alloys with Ni or Cu or Au/Ni/Cu substrates [5,11–22], and several literatures had regarded with interfacial reactions and the mechanical properties of Sn–Ag–Cu alloys by adding a minor amount of Ni or Ge elements to the Au/Ni/Cu substrate [8,21,24–31]. The Sn–4.0Ag0.5–Cu alloy is one of popular lead-free solders and the Au/Ni/Cu multi-layer is the common UBM structure in electronic packaging. To ensure the solder joint reliability, a clearer understanding of the solder joint strength and interfacial reactions, including the reaction kinetics, intermetallic compound (IMC) growth mechanism, in the Sn–Ag–Cu/Au/Ni/Cu and Sn–Ag–Cu–Ni–Ge/Au/Ni/Cu couples is necessary. In this study, the Sn–4.0Ag0.5–Cu/Au/Ni/Cu and Sn–4.0Ag–0.5Cu–0.05Ni–0.01Ge/Au/Ni/Cu couples were reflowed and aged at various temperatures for different periods of the reaction time. The evolution and reaction mechanism of the IMCs, which were formed at the interface, were investigated. The joint strength was determined, as well.

2. Experimental procedures

Commercial Sn–4.0 wt%Ag–0.5 wt%Cu (SAC) and Sn–4.0 wt%Ag–0.5 wt%Cu–0.05 wt%Ni–0.01 wt%Ge (SACNG) lead-free solders of 600 μm diameter were used in this study. The liquidus temperature was measured using a

* Corresponding author at: Department of Materials Science and Engineering, National Taiwan University of Science and Technology, 43 Keelung Road, Section 4, Taipei 10672, Taiwan, ROC. Tel.: +886 2 27376659; fax: +886 2 27301265.
E-mail address: ywyen@mail.ntust.edu.tw (Y.-W. Yen).

0925-8388/$ – see front matter © 2011 Elsevier B.V. All rights reserved.
doi:10.1016/j.jallcom.2011.01.114

Table 1
Liquidus temperature and wetting time for the SAC and SACNG solders.

	SAC	SACNG
T_l (°C)	220.9	219.7
Wetting time (s)	0.85	0.75

differential scanning calorimeter. The wetting time was determined using a solder checker. The liquidus temperature and wetting time are listed in Table 1. Quite similar properties between the SAC and SACNG solders are found in Table 1. It indicates that Ni and Ge atoms added to the SAC solder would not significantly change its liquidus temperature and wetting time. A 450 μm × 450 μm Cu pad, which was coated with the Au(1 μm)/Ni(25 μm) layers on it, was used. The solder ball was placed onto the metallic pad in a furnace at 240 and 255 °C for 3, 5, 10, and 20 min for reflowing. The reflowed specimens were subsequently treated by thermal aging in a furnace at 150 °C for 100–500 h.

After the reaction, each specimen was metallographically prepared to inspect the cross-section micrograph. An optical microscope (OM) and scanning electron microscope (SEM) were used to examine the surface morphology. If there were IMCs formed at the interface, the quantitative chemical analysis of the IMC was performed using SEM with an energy dispersion spectrometer (EDS) and electron probe micro-analyzer (EPMA).

The shear stress of each specimen was examined using a universal test machine to evaluate the solder joint strength. The universal test machine with a constant speed 200 μm/s prodded the specimen until the solder ball was totally removed from the metallic pad. The morphology of the fractured surface was inspected using SEM to demonstrate the cause of the fracture.

3. Results and discussion

3.1. Interfacial reactions in the SAC/Au/Ni/Cu couple

Fig. 1(a) shows the backscattered electron image (BEI) of the SAC/Au/Ni/Cu couple reflowed at 240 °C for 3 min. During the reflow process, the Au layer was completely dissolved into the molten solder. However, the Ni layer was still observed. It had not yet been consumed thoroughly during this process. Based on the composition analysis using EPMA and SEM/EDS, two IMCs were observed at the interface and in the solder, respectively. Close to the Ni side, a planar layer IMC with Sn–21.32 at.%Ni–33.67 at.%Cu and minor Au about 0.32 at.% composition was formed. It is likely to be the (Cu, Ni, Au)$_6$Sn$_5$ phase [13,32]. Because the Cu, Ni and Au elements have the same face-centered cubic (FCC) structure, the Ni and Au atoms can incorporate into the sublattice of the Cu$_6$Sn$_5$ phase to form the (Cu, Ni, Au)$_6$Sn$_5$ phase [13,32]. An IMC with an irregular shape was observed in the solder. It should be the AuSn$_4$ phase of Au–82.32 at.% Sn [32]. Fig. 1(b) shows the BEI micrograph of the SAC/Au/Ni/Cu couple reflowed at 240 °C for 10 min. The AuSn$_4$ phase was still observed in the solder. However, a two layer IMC structure was formed at the SAC/substrate interface. This structure consisted of the (Cu, Ni, Au)$_6$Sn$_5$ phase which was close to the SAC solder and the (Ni, Cu, Au)$_3$Sn$_4$ phase which was close to the Ni side [13,32]. This result indicated that an increase in reflowing time can influence the IMC formation.

In the initial reflowing stage, the Cu atoms from the solder rapidly reacted with the Ni substrate. The Cu concentration near the substrate was high enough to form the (Cu, Ni, Au)$_6$Sn$_5$ phase on the Ni surface, although the Ni layer still remained on the Cu surface [13]. The Ni atoms from the substrate continuously dissolved into the solder with increasing the reflowing time. This would dilute the Cu concentration in the molten solder. Thus, the Cu concentration near the substrate was not sufficient to form the (Cu, Ni, Au)$_6$Sn$_5$ phase at the interface. According to the Sn–Ni–Cu ternary diagram [7] and Kao's study [13], the equilibrium condition should be in the Cu$_6$Sn$_5$–Ni$_3$Sn$_4$–L tie-triangle. When the reflowing time was increased, the decrease in the Cu concentration in the molten solder occurred. Therefore, the equilibrium phase region would shift into a tie-triangle composed of the Cu$_6$Sn$_5$–Ni$_3$Sn$_4$–L region from the two-phase region, Cu$_6$Sn$_5$–L region. That is why

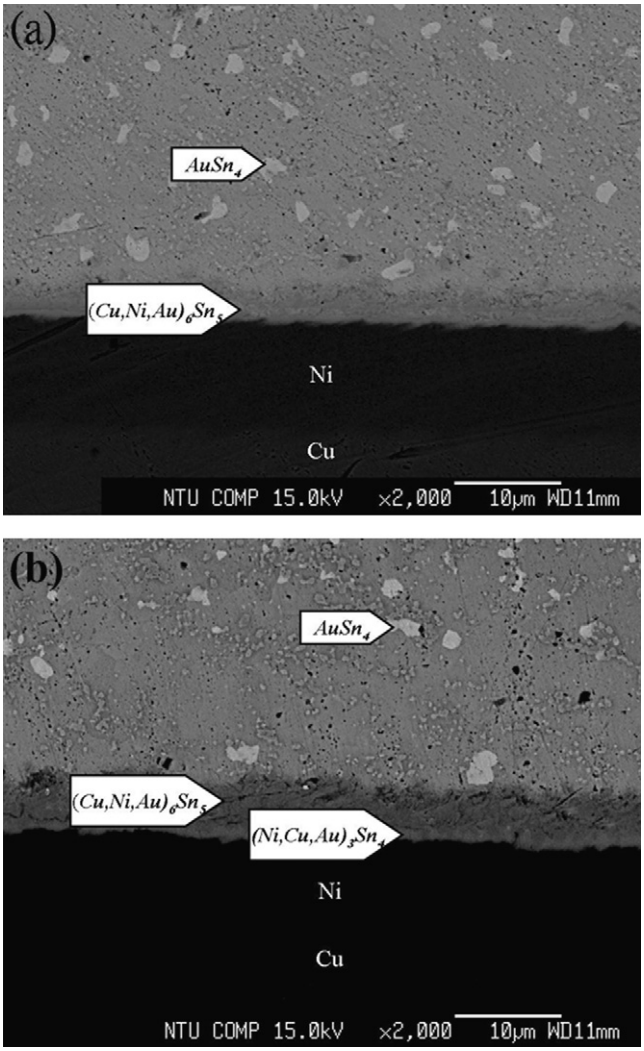

Fig. 1. BEI micrographs of the SAC/Au/Ni/Cu couples reflowed at 240 °C for (a) 3 min and (b) 10 min.

the (Cu, Ni, Au)$_6$Sn$_5$ and (Ni, Cu, Au)$_3$Sn$_4$ phases were formed at the interface.

Fig. 2(a) and (b) shows BEI micrographs of the SAC/Au/Ni/Cu couple reflowed at 240 °C for 3 and 10 min and consequently aged at 150 °C for 500 h. After taking a long period of heat-treatment at 150 °C, the (Cu, Ni, Au)$_6$Sn$_5$ phase was formed at the interface in the SAC/substrate couple reflowed for 3 min. The (Cu, Ni, Au)$_6$Sn$_5$ and (Ni, Cu, Au)$_3$Sn$_4$ phases were observed at the interface in the SAC/Au/Ni/Cu couple reflowed for 10 min. These IMC evolutions at the interface in Fig. 2(a) and (b) are very similar to those in Fig. 1(a) and (b). The results indicate that long-term heat aging did not affect the IMC formation at the interface. However, the IMC thickness in both couples for different reflowing times was increased as the aging time was increased. Fig. 3 presents the relationship between the IMC thickness and the square root of the aging time. A linear relation is found in Fig. 3. It reveals that the IMC growth mechanism in both couples was diffusion-controlled. The growth constant (k) is listed in Table 2. When the reflowing temperature is raised to 255 °C or the aging time is increased to 500 h, similar results are found in Fig. 3. The growth rate constant is increased as the aging temperature is increased.

Why does the (Cu, Ni, Au)$_6$Sn$_5$ phase not transform into the (Cu, Ni, Au)$_6$Sn$_5$ and (Ni, Cu, Au)$_3$Sn$_4$ phases through long periods of heat-treatment at 150 °C? It is likely that the Cu diffusion rate in

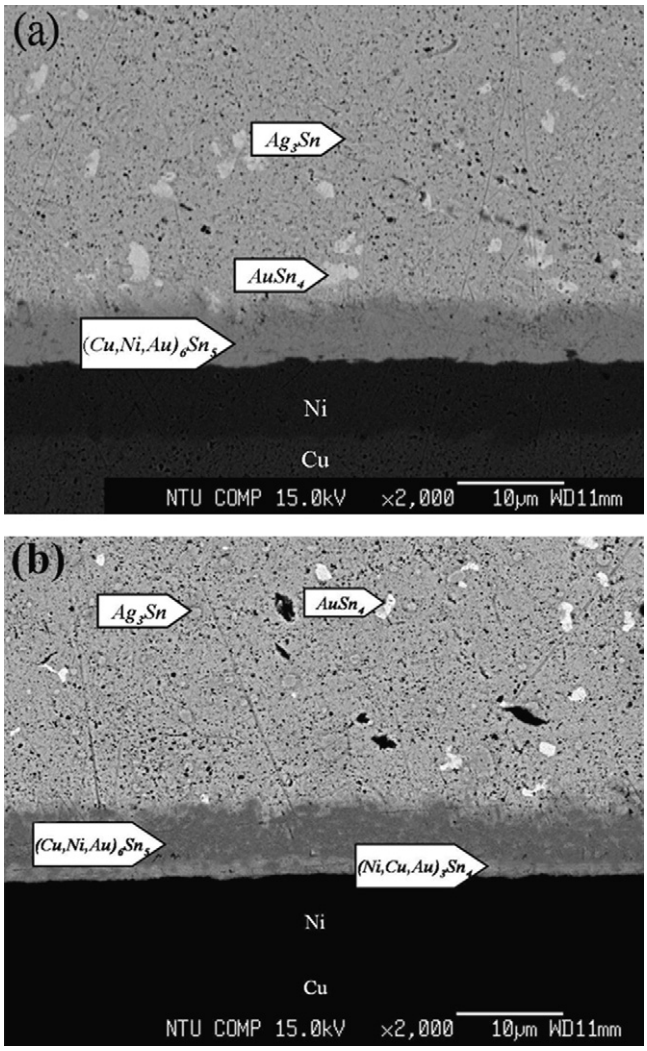

Fig. 2. BEI micrographs of the SAC/Au/Ni/Cu couples reflowed at 240 °C for (a) 3 min and (b) 10 min and then aged at 150 °C for 500 h.

Table 2
Growth rate constants ($k \times 10^{14}$ m^2/s) for the SAC/Au/Ni/Cu and SACNG/Au/Ni/Cu couples.

System	Temperature-reflowing time			
	240-03	240-10	255-03	255-10
SAC405/Au/Ni/Cu	1.15	3.86	1.20	4.68
SACNG/Au/Ni/Cu	5.21	19.01	20.02	79.01

the solid–solid reaction is slow enough to cause a deficiency in a Cu concentration near the interface. The Cu and Ni concentrations remain in the initial reflowing condition. This means that the equilibrium condition does not change. The Ag_3Sn and $AuSn_4$ phases

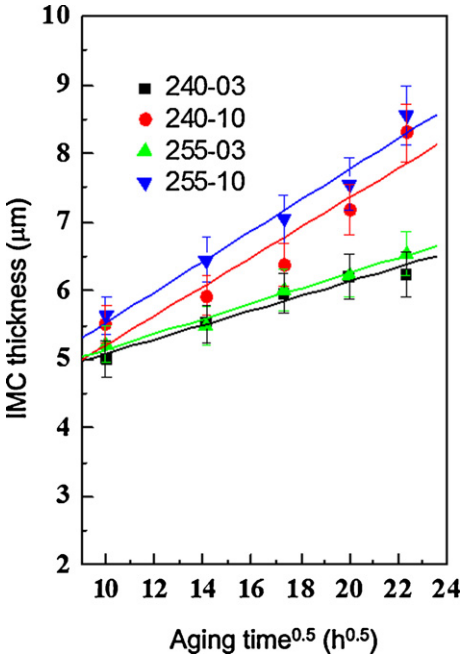

Fig. 3. Thickness of IMC layer in the SAC/Au/Ni/Cu couple.

were still observed in the solder, as shown in Fig. 2(a) and (b). However, the $AuSn_4$ phases vanished gradually with the increase in aging time. According to Ho et al.'s study, the $AuSn_4$ phases preferred to alloy with Ni atoms and segregated toward the interface to form a $(Au_{1-x}Ni_x)Sn_4$ layer in the interfacial reaction [33]. Sharif et al. indicated that the affinity of Ni atoms with Sn–Cu IMCs was better than that with Sn–Au IMCs [34]. Thus, the Sn–Cu compound close to the Ni side formed the (Cu, Ni, Au)$_6$Sn$_5$ phase at the interface easier than the $(Au_{1-x}Ni_x)Sn_4$ phase. The Au content in the (Cu, Ni, Au)$_6$Sn$_5$ phase increased with the increase in aging time.

3.2. Interfacial reactions in the SACNG/Au/Ni/Cu couple

Fig. 4(a) shows the BEI micrograph of the SACNG/Au/Ni/Cu couple reflowed at 240 °C for 3 min. According to the EPMA chemical analysis, a continuous (Cu, Ni, Au)$_6$Sn$_5$ layer at the interface and the $AuSn_4$ phase within the solder were observed. With the increase in reflowing time to 10 min, two IMCs layers, the (Cu, Ni, Au)$_6$Sn$_5$ and (Ni, Cu, Au)$_3$Sn$_4$ phases, were observed at the solder/substrate interface, as shown in Fig. 4(b). Fig. 5(a) and (b) shows BEI micrographs of the SACNG/Au/Ni/Cu couple reflowed at 240 °C for 3 min and 10 min and then aged at 150 °C for 500 h, respectively. The (Cu, Ni, Au)$_6$Sn$_5$ phase was formed at the interface in the 3-min reflowing case. The (Cu, Ni, Au)$_6$Sn$_5$ and (Ni, Cu, Au)$_3$Sn$_4$ phases were formed between the solder and substrate in the SACNG/Au/Ni/Cu couple reflowed for 10 min and aged for 500 h. The Ag_3Sn and $AuSn_4$ phases were still observed in the solder. Fig. 6 shows that the total IMC thickness increased with the increase in aging time. A linear

Table 3
Evolution of IMCs formed at the interface in two reaction couples reflowed and then aged at various temperatures and times.

Reaction couples	Aging time (h)	Reflowing conditions			
		240 °C		255 °C	
		3 min	10 min	3 min	10 min
SAC/Au/Ni/Cu	100–500	(Cu, Ni, Au)$_6$Sn$_5$	(Cu, Ni, Au)$_6$Sn$_5$ (Ni, Cu, Au)$_3$Sn$_4$	(Cu, Ni, Au)$_6$Sn$_5$	(Cu, Ni, Au)$_6$Sn$_5$ (Ni, Cu, Au)$_3$Sn$_4$
SACNG/Au/Ni/Cu	100–500	(Cu, Ni, Au)$_6$Sn$_5$	(Cu, Ni, Au)$_6$Sn$_5$ (Ni, Cu, Au)$_3$Sn$_4$	(Cu, Ni, Au)$_6$Sn$_5$	(Cu, Ni, Au)$_6$Sn$_5$ (Ni, Cu, Au)$_3$Sn$_4$

Table 4
Shear stress values and ratio (R) of the SAC/substrate joints in different reflowing and aging conditions.

Reflowing temperature (°C)	Reflowing time (min)	Shear tress after 100 h-aging			Shear stress after 500 h-aging		
		τ_0 (N/mm^2)	τ (N/mm^2)	R (%)	τ_0 (N/mm^2)	τ (N/mm^2)	R (%)
240	3	12.8	10.3	80.2	12.8	8.9	69.5
240	10	12.4	10.50	84.7	12.4	8.9	71.2
255	3	12.6	9.8	78.0	12.6	9.6	75.8
255	10	12.1	10.0	83.0	12.1	8.9	73.5

Table 5
Shear stress values and ratio (R) of the SACNG/substrate joints in different reflowing and aging conditions.

Reflowing temperature (°C)	Reflowing time (min)	Shear tress after 100 h-aging			Shear stress after 500 h-aging		
		τ_0 (N/mm^2)	τ (N/mm^2)	R (%)	τ_0 (N/mm^2)	τ (N/mm^2)	R (%)
240	3	12.2	10.1	82.6	12.2	9.8	79.9
240	10	12.5	10.2	82.0	12.5	9.9	79.6
255	3	12.3	10.5	85.2	12.3	10.2	82.7
255	10	12.4	10.1	81.9	12.4	10.0	80.92

relationship is found between the aging time and IMC thickness. This means that the IMC growth mechanism is diffusion-controlled. The growth rate constants in the SACNG/substrate couples are listed in Table 2. The k value is increased as the aging temperature is increased in the SACNG/substrate couples. These results are similar to that in the SAC/substrate couples and literature data [25,26].

The IMC evolution in both couples is listed in Table 3. The results in the SACNG/Au/Ni/Cu couple were similar to those in the SAC/Au/Ni/Cu couples. In all couples, IMCs with no Ge solu-

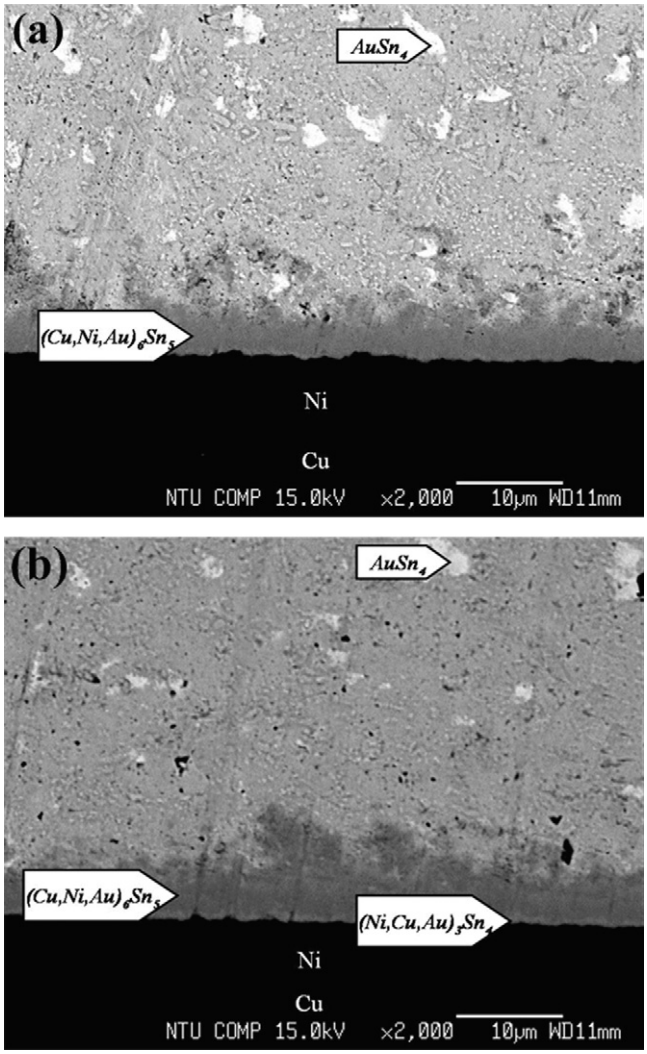

Fig. 4. BEI micrographs of the SACNG/Au/Ni/Cu couples reflowed at 240 °C for (a) 3 min and (b) 10 min.

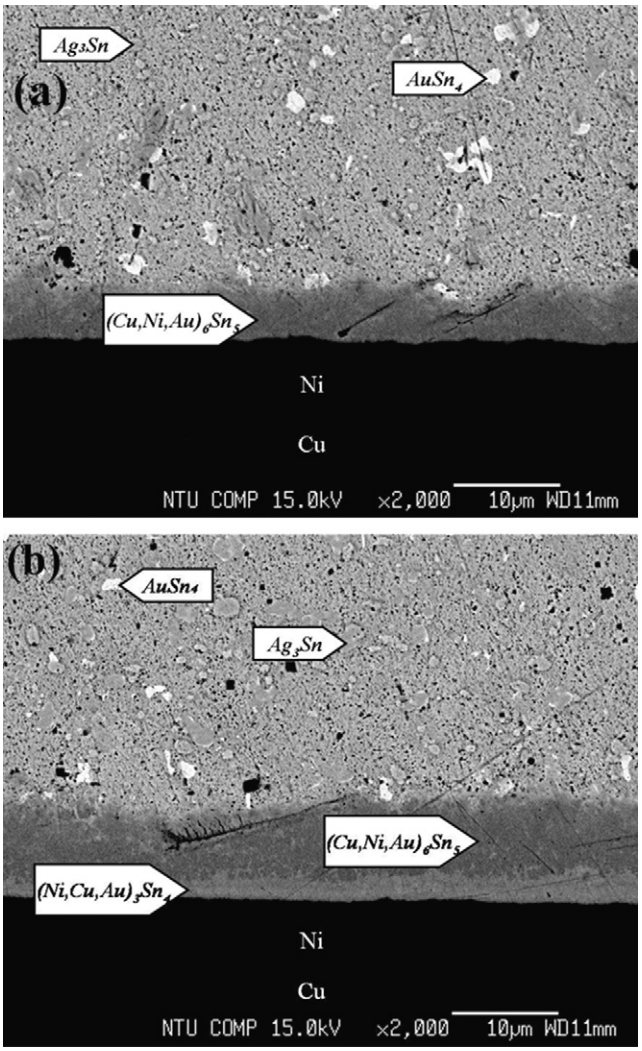

Fig. 5. BEI micrographs of the SACNG/Au/Ni/Cu couples reflowed at 240 °C for (a) 3 min and (b) 10 min and then aged at 150 °C for 500 h.

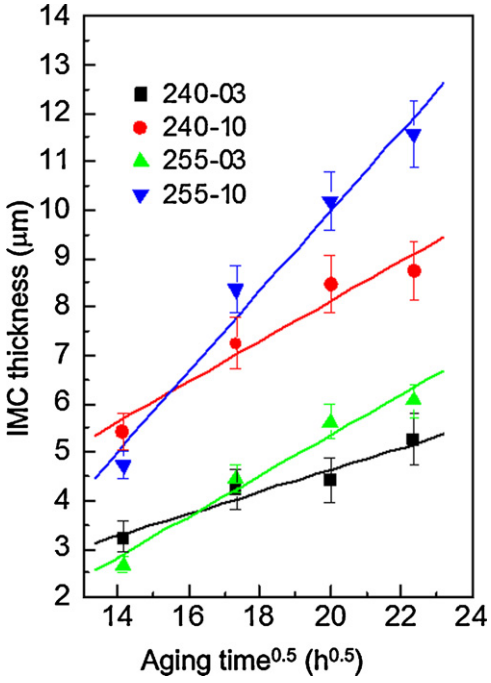

Fig. 6. Thickness of IMC layer in the SACNG/Au/Ni/Cu couples.

bility were formed at the interface. However, based on Table 2, the growth rate constant in the SACNG/substrate couples is always greater than that in the SAC/substrate couples. The addition of Ni and Ge into the SAC solder would not significantly change the IMC formation in the solder/substrate couples but it seems to accelerate the interfacial growth rate in the solder/substrate system.

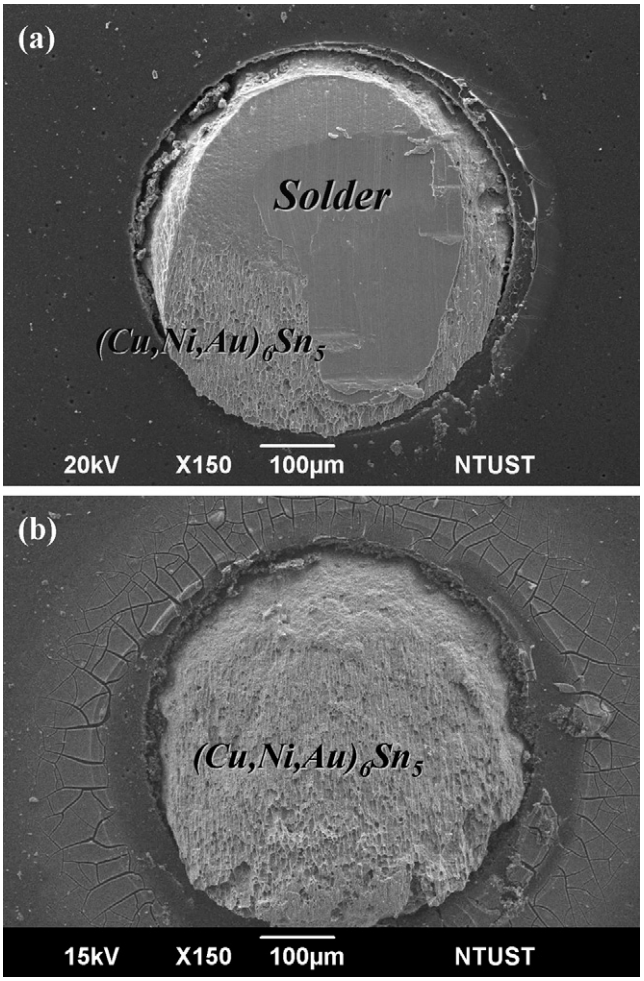

Fig. 8. Fracture surface morphologies of the SAC/Au/Ni/Cu couple aged at 150 °C for (a) 300 h and (b) 400 h.

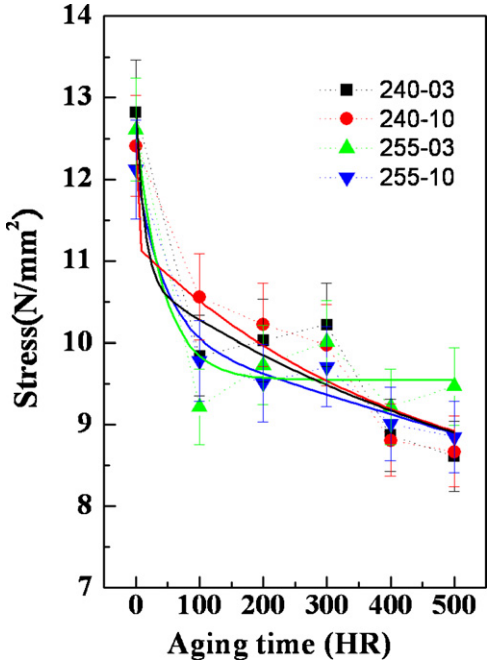

Fig. 7. Shear strength of the SAC/Au/Ni/Cu couple under different reflow conditions (■: at 240 °C for 3 min; ●: at 240 °C for 10 min; ▲: at 255 °C for 3 min; ▼: at 255 °C for 10 min), and then aged at 150 °C for 500 h.

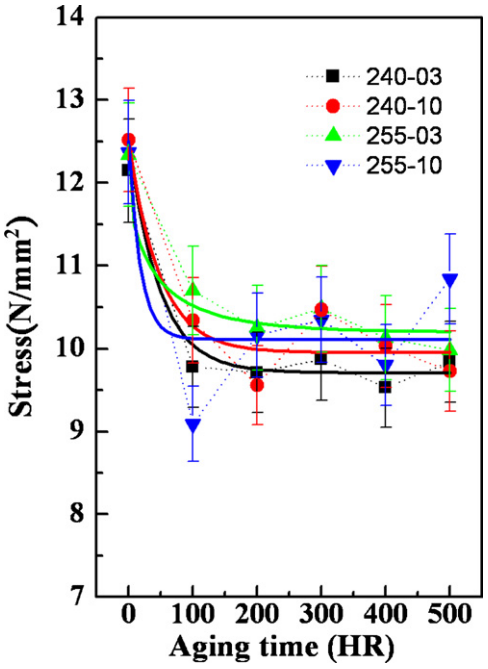

Fig. 9. Shear strength of the SACNG/Au/Ni/Cu couple under different reflow conditions (■: at 240 °C for 3 min; ●: at 240 °C for 10 min; ▲: at 255 °C for 3 min; ▼: at 255 °C for 10 min), and then aged at 150 °C for 500 h.

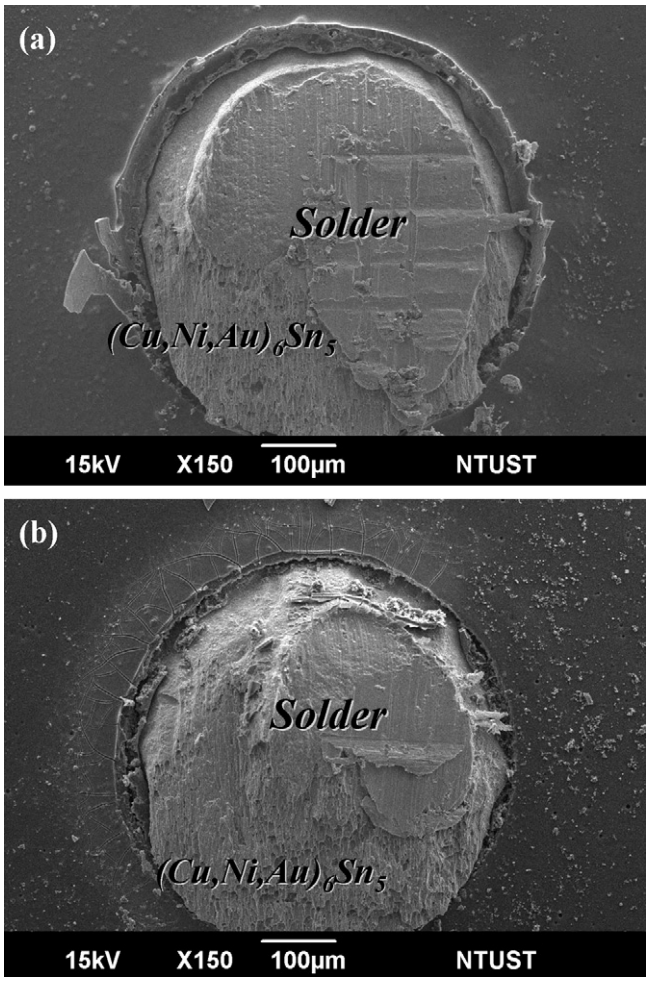

Fig. 10. Fracture surface morphologies of the SACNG/Au/Ni/Cu couple aged at 150 °C for (a) 300 h and (b) 400 h.

3.3. Mechanical properties in the SAC/Au/Ni/Cu and SACNG/Au/Ni/Cu couples

A shear stress test was carried out to evaluate the Ni and Ge addition effect to the SAC solder on the solder joints. The shear stress ratio (R) in this study is defined as,

$$R\ (\%) = \frac{\tau}{\tau_0} \times 100$$

where τ is the shear stress value after the aging process and τ_0 is the initial shear stress value. Fig. 7 displays the shear stress values for the SAC/Au/Ni/Cu joints under four different reflowing conditions: [1] at 240 °C for 3 min; (2) at 240 °C for 10 min; (3) at 255 °C for 3 min; and (4) at 255 °C for 10 min, and then aged at 150 °C for 100–500 h. The shear stress values of these solder joints in each specimen declined abruptly within the 100-h-aging treatment and then decreased slowly after 100-h-aging treatment. The detailed shear stress values are listed in Table 4. Based on Table 4, the strength ratio (R) of the aged specimens at 150 °C for 100 h was approximately 81% and the strength ratio of the aged specimens at 150 °C for 500 h was approximately 72%. Therefore, the strength of the aged specimens declined dramatically from the 0–100 h aging time. Subsequently, the strength of the aged specimens did not be deteriorated effectively with the longer aging time after 100 h-aging.

Fig. 8 shows the fracture surface morphologies of the SAC/Au/Ni/Cu couple reflowed at 240 °C for 10 min then aged at 150 °C for (a) 300 h and (b) 400 h after the shear stress test. The specimen aged for 300 h presents a smooth fractured plane along the solder and the IMCs, as shown in Fig. 8(a). With the aging time increased to 400 h, the specimen fracture surface was transferred to the IMC–IMC interface instead of the solder–IMC interface on the solder joint surface. The fracture type changed from a ductile fracture into a brittle fracture contributed by the thicker (Cu, Ni, Au)$_6$Sn$_5$ phase formed at the interface. This might be the reason for the deterioration in the shear stress.

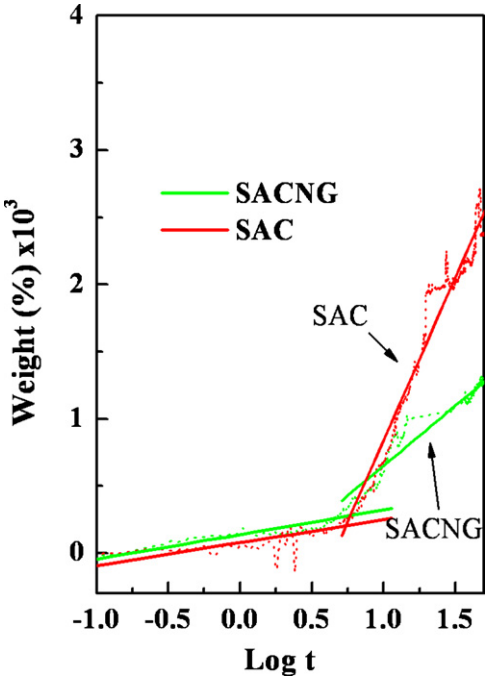

Fig. 11. TGA analyses of the SAC and SACNG solders.

Fig. 9 displays the shear strength of the solder joint at the SACNG/substrate interface under the same reflowing and aging conditions. The shear stress values in the SACNG/substrate interface declined abruptly at an aging time of 100 h, and then decreased slowly over the aging time of 100 h. Fig. 9 also presents that the shear stress ratio (R) of the specimen aged at 150 °C for 100 h approximately is 81–85% and that at 150 °C for 500 h-aging approximately is 79–82%. The detailed values are listed in Table 5. The SACNG/substrate solder joint results are similar to those in the SAC/substrate solder joints. According to Figs. 7 and 9, the shear stress of both SAC/Au/Ni/Cu and SACNG/Au/Ni/Cu couples were close to 12.50 N/mm^2 at the beginning. However, with increased aging time from 100 to 500 h, the slope of the shear stress versus the aging time in the SAC/Au/Ni/Cu couple was larger than that in the SACNG/Au/Ni/Cu couple. This revealed that a minor addition of Ni and Ge to the SAC solder could improve the solder joint mechanical strength.

Fig. 10 shows the fracture surface morphologies of the solder joint in the SACNG/Au/Ni/Cu coupled aged at 150 °C for (a) 300 h and (b) 400 h after the shear stress test. A smooth fracture plane was observed along the solder–IMC interface in both solder joints, as shown in Fig. 10(a) and (b). These two fracture surface regions were composed of the solder and (Cu, Ni, Au)$_6$Sn$_5$ phase determined using EDS analysis. The fracture interface in the SACNG/Au/Ni/Cu solder joint did not change from the solder–IMC interface to the IMC–IMC interface as the aging time was increased to 400 h. The SACNG/Au/Ni/Cu solder joint fracture was always a ductile fracture. This result is consistent with Meng et al.' study [27]. However, the IMC–IMC fracture morphology and brittle fracture type were found

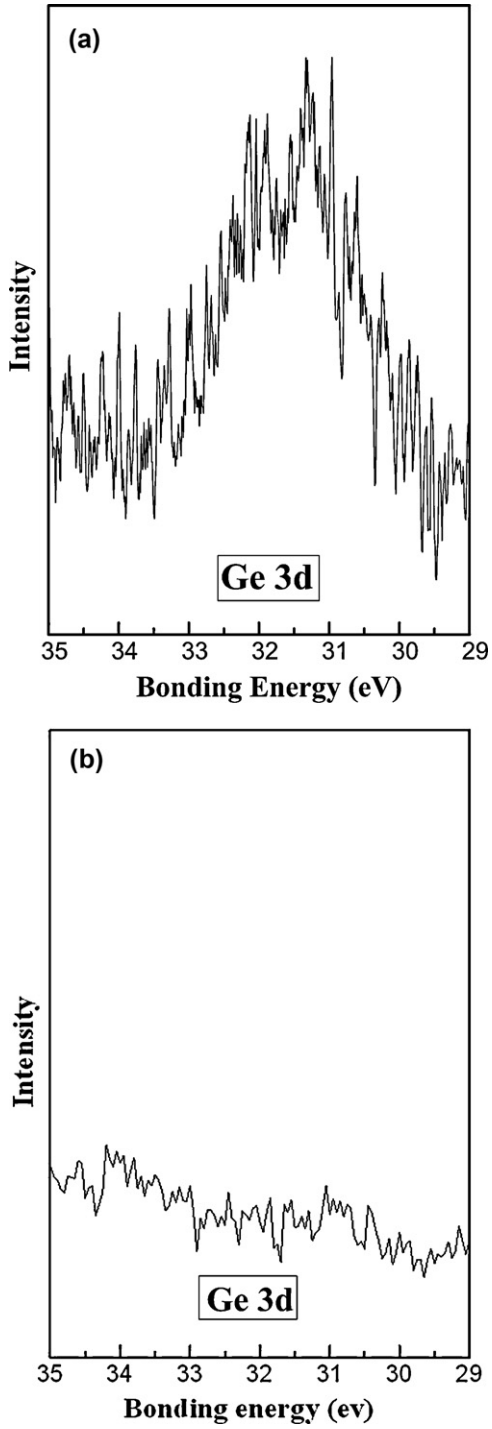

Fig. 12. XPS analysis results in the (a) SACNG and (b) SAC solder surface.

in the SAC/Au/Ni/Cu solder joint after 400 h-aging. That is why the SACNG/Au/Ni/Cu solder joint has better mechanical strength than the SAC/Au/Ni/Cu solder joint. Several studies had similar results [23–25,27–31].

The better mechanical strength of the SACNG/Au/Ni/Cu solder joint is contributed from the SACNG solder which has a superior anti-oxidation ability [6,31]. According to the previous study, oxidation is a harmful problem that decreases the bonding strength in solder joints [8]. Fig. 11 shows the thermo-gravimetric analysis (TGA) curves for SAC and SACNG solders. The result in Fig. 11 displays that the SACNG solder gained lesser weight increase than the

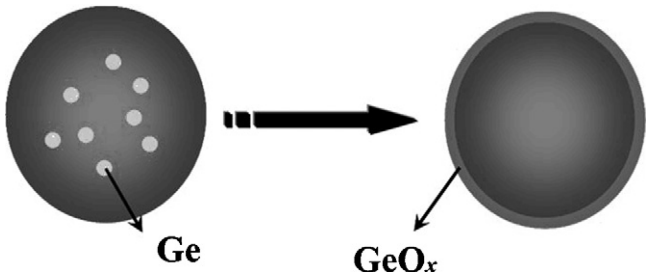

Fig. 13. Schematic diagram of the Ge element segregation in the SACNG solder.

SAC solder. This means that less oxidation was formed in the SACNG solder than in the SAC solder. This was consistent with the SACNG solder, which had a good anti-oxidation ability. The X-ray photoelectron spectroscopy/electron spectroscopy for chemical analysis (XPS/ESCA) for the SACNG solder indicated that the Ge element signal can only be detected on the SACNG solder surface. Fig. 12 shows the XPS analysis results in the (a) SACNG and (b) SAC solder surface. It obviously found that there was the Ge single in Fig. 12(a). On the other hand, there no the Ge single could be found in Fig. 12(b). The detection limit of the XPS/ESCA is 0.1 at.%. The Ge concentration in the SACNG solder is 0.01 wt% which is equal to 0.016 at.%. Thus, if the Ge single can be detected by the XPS/ESCA, it means that the Ge element must completely segregate to the solder surface. It is probable that the Ge element added to the SAC solder was consumed to form a GeO_x thin layer on the solder surface. Fig. 13 shows a schematic diagram of the Ge element segregation in the SACNG solder. The density of the Ge and Sn elements is 5.32 and 7.28 g/cm^3, respectively. There is a large difference in density between the Ge and Sn elements. After reflowing, the Ge element easily segregates toward the surface of the SACNG solder to form a thin oxide layer. This thin oxide layer acts as a protective layer to prevent oxygen from the air reacting with the solder to form a SnO_x layer and improves the wettability between the solder and substrate. This could explain why the shear stress in the SACNG/Au/Ni/Cu solder joints is greater than that in the SAC/Au/Ni/Cu solder joints. According to this characteristic, the SACNG solder is a good choice to solve the oxidation problem and it can increase the bonding strength during the soldering process.

4. Conclusions

Two lead-free solders, Sn–4.0Ag–0.5Cu (SAC) and Sn–4.0Ag–0.5Cu–0.05Ni–0.01Ge (SACNG), reacting with a multilayer Au/Ni/Cu substrate were investigated in this study. The following conclusions are summarized:

1. Only the $(Cu, Ni, Au)_6Sn_5$ phase was formed in the SAC/Au/Ni/Cu and SACNG/Au/Ni/Cu couples reflowed at 240 and 255 °C for 3 min, even aged at 150 °C for 500 h. When the reflowing time was increased to 10 min, both the $(Cu, Ni, Au)_6Sn_5$ and $(Ni, Cu, Au)_3Sn_4$ phases were formed at the interface. The IMC formation did not change when these couples were then aged at 150 °C for 500 h. With increasing aging time, the $AuSn_4$ and Ag_3Sn phases were observed in the solders. All of the IMC thicknesses obeyed the parabolic law. The IMC growth mechanism in these couples is diffusion-controlled.
2. The shear strength of the SACNG/Au/Ni/Cu couple was higher than that of the SAC/Au/Ni/Cu couple. It was likely that the fractured surface of the SACNG/Au/Ni/Cu couple was the solder–IMC interface and the failure model was a ductility failure. However, the fractured surface of the SAC/Au/Ni/Cu couple was IMC–IMC interface and it was a brittle failure.

3. The addition of Ni and Ge into the SAC solder does not influence the interfacial reaction. However, it has a great contribution to increase shear strength owing to the aggregation of Ge on the solder ball surface which enhances anti-oxidation ability.

Acknowledgements

The authors acknowledge the financial support of the National Science Council of Taiwan, Republic of China (Grant No. NSC 99-2628-E-011-009) and Mr. Laiw for FE-SEM operation and Mr. C.Y. Kao for carrying out the EPMA analysis.

References

[1] E.P. Eood, K.L. Nimmo, J. Electron. Mater. 23 (1997) 709–713.
[2] M.D. Settle, C.C. Patterson, Science 24 (1980) 21–23.
[3] M.M. Comack, S. Jin, J. Electron. Mater. 23 (1994) 715–720.
[4] D.R. Smith, A.R. Flegal, AMBIO 24 (1995) 21–23.
[5] S.W. Chen, Y.W. Yen, J. Electron. Mater. 28 (1999) 1203–1208.
[6] J.W. Yoon, S.B. Jung, J. Alloys Compd. 396 (2005) 122–127.
[7] J.W. Yoon, S.W. Kim, S.B. Jung, J. Alloys Compd. 392 (2005) 247–252.
[8] S.W. Cho, K. Han, Y. Yi, S.J. Kang, K.H. Yoo, K. Jeong, C.N. Whang, Adv. Eng. Mater. 8 (2006) 111–114.
[9] Y.D. Jeon, S. Nieland, A. Ostmann, H. Reichl, K.W. Paik, J. Electron. Mater. 32 (2003) 548–557.
[10] K. Yokomine, N. Shimizu, Y. Miyamoto, Y. Iwata, D. Love, K. Newman, Proc. Electron. Comp. Technol. Conf. (2001) 13484–21392.
[11] S.K. Kang, V. Ramachandran, Scr. Metall. 14 (1980) 421–424.
[12] S. Bader, W. Gust, H. Hieber, Acta Metall. Mater. 43 (1995) 329–337.
[13] D. Gur, M. Bamberger, Acta Mater. 46 (1998) 4917–4923.
[14] S.W. Chen, C.M. Chen, W.C. Liu, J. Electron. Mater. 27 (1998) 1193–1198.
[15] C.M. Liu, C.E. Ho, W.T. Chen, C.R. Kao, J. Electron. Mater. 30 (2001) 1152–1156.
[16] C.E. Ho, L.C. Shiau, C.R. Kao, J. Electron. Mater. 31 (2002) 1264–1269.
[17] C.E. Ho, R.Y. Tsai, Y.L. Lin, C.R. Kao, J. Electron. Mater. 31 (2002) 584–590.
[18] F. Zhang, M. Li, C.C. Chum, Z.C. Shao, J. Electron. Mater. 32 (2003) 123–130.
[19] W.C. Luo, C.E. Ho, J.Y. Tsai, Y.L. Lin, C.R. Kao, Mater. Sci. Eng. A 396 (2005) 385–391.
[20] C.H. Wang, S.W. Chen, Acta Mater. 54 (2006) 247–253.
[21] T.H. Chuang, S.F. Yen, M.D. Cheng, J. Electron. Mater. 315 (2006) 385–391.
[22] C.E. Ho, S.C. Yang, C.R. Kao, J. Mater. Sci.: Mater. Electron. 18 (2006) 155–174.
[23] I. Shohji, S. Tsunoda, H. Watanabe, T. Asai, Key Eng. Mater. 353–358 (2007) 2033–2036.
[24] I. Shohji, H. Watanabe, T. Okashita, T. Osawa, Mater. Trans. 49 (2008) 1513–1517.
[25] Y.S. Lai, J.M. Song, H.C. Chang, Y.T. Chiu, J. Electron. Mater. 37 (2008) 201–209.
[26] K.L. Lin, P, O. Shih, J. Alloys Compd. 452 (2008) 291–297.
[27] G. Meng, C. Li, T. Yang, L. Chen, Hanjie Xuebao/Trans. China Weld. Inst. 29 (2008) 59–62.
[28] M. Yamashita, N. Hidaka, I. Shohji, 10th Electronics Packaging Technology Conference (EPTC), 2008, pp. 582–587.
[29] N. Hidaka, H. Watanabe, M. Yoshiba, J. Electron. Mater. 38 (2009).
[30] M. Shimoda, N. Hidaka, M. Yamashita, K. Sakaue, T. Ogawa, Proceedings of the Electronic Packaging Technology Conference (EPTC), 2009, pp. 725–730.
[31] E.P. Leng, W.T. Ling, N. Amin, I. Ahmad, T.Y. Han, C.W. Chiao, A.S.M.A. Haseeb, Proceedings of the Electronic Packaging Technology Conference (EPTC), 2009, pp. 82–91.
[32] H. Baker (Ed.), ASM Handbook—Alloy Phase Diagram, vol. 3, ASM International, Materials Park, OH, 1992, pp. 2.78, 2.178, 2.318.
[33] C.E. Ho, W.T. Chen, C.R. Kao, J. Electron. Mater. 30 (2001) 379–387.
[34] A. Sharif, M.N. Islam, Y.C. Chan, Mater. Sci. Eng. B 113 (2004) 184–189.